Intrathecal Adeno-Associated Viral Vector-Mediated Gene Delivery for Adrenomyeloneuropathy

Yi Gong,[1] Anna Berenson,[1] Fiza Laheji,[1] Guangping Gao,[2] Dan Wang,[2] Carrie Ng,[1] Adrienn Volak,[1] Rene Kok,[1,3] Vasileios Kreouzis,[1] Inge M. Dijkstra,[3] Stephan Kemp,[3] Casey A. Maguire,[1] and Florian Eichler[1,*]

[1]Department of Neurology, Massachusetts General Hospital, Harvard Medical School, Boston, Massachusetts; [2]Horae Gene Therapy Center, University of Massachusetts Medical School, Worcester, Massachusetts; and [3]Departments of Clinical Chemistry and Pediatrics, Academic Medical Center, University of Amsterdam, Amsterdam, the Netherlands.

Mutations in the gene encoding the peroxisomal ATP-binding cassette transporter (*ABCD1*) cause elevations in very long-chain fatty acids (VLCFAs) and the neurodegenerative disease adrenoleukodystrophy (ALD). In most adults, this manifests as the spinal cord axonopathy adrenomyeloneuropathy (AMN). A challenge in virus-based gene therapy in AMN is how to achieve functional gene correction to the entire spinal cord while minimizing leakage into the systemic circulation, which could contribute to toxicity. In the present study, we used an osmotic pump to deliver adeno-associated viral (AAV) vector into the lumbar cerebrospinal fluid space in mice. We report that slow intrathecal delivery of recombinant AAV serotype 9 (rAAV9) achieves efficient gene transfer across the spinal cord and dorsal root ganglia as demonstrated with two different transgenes, *GFP* and *ABCD1*. In the *Abcd1*$^{-/-}$ mouse, gene correction after continuous rAAV9-CBA-h*ABCD1* delivery led to a 20% decrease in VLCFA levels in spinal cord compared with controls. The major cell types transduced were astrocytes, vascular endothelial cells, and neurons. Importantly, rAAV9 delivered intrathecally by osmotic pump, in contrast to bolus injection, reduced systemic leakage into peripheral organs, particularly liver and heart tissue.

Keywords: adrenoleukodystrophy, gene therapy, adeno-associated viral vector, adrenomyeloneuropathy, intrathecal, central nervous system

INTRODUCTION

X-LINKED ADRENOLEUKODYSTROPHY (ALD) is a debilitating neurological disorder caused by mutations in the *ABCD1* gene.[1] This gene encodes the peroxisomal ATP-binding cassette (ABC) transporter responsible for transporting CoA-activated very long-chain fatty acids from the cytosol to peroxisomes for further degradation.[1,2] Therefore, one of the significant biochemical hallmarks of ALD is the accumulation of straight-chain saturated very long-chain fatty acids (VLCFAs: $C_{24:0}$ and $C_{26:0}$) and monounsaturated VLCFAs ($C_{26:1}$) in the plasma and other tissues.[3,4]

ALD has two distinct neurological phenotypes: childhood cerebral adrenoleukodystrophy, which manifests in males as progressive behavioral and cognitive neurological deficits as well as inflammatory brain demyelination that leads to total disability in the first decade; and the more common AMN, which presents in males and females as a slowly progressive paraparesis and distal axonopathy of the spinal cord that is compatible with survival into the eighth decade.[5,6] So far, hematopoietic stem cell transplantation and stem cell-based gene therapy are the only modalities able to halt the progressive cerebral demyelination.[7,8] However, AMN, which develops in 60% of the patients with ALD, is currently still left without available treatment options.[9,10]

Recombinant adeno-associated viral (rAAV) vector-mediated gene therapy has shown great promise in several clinical trials for neurological

*Correspondence: Dr. Florian S. Eichler, Department of Neurology, Massachusetts General Hospital, Harvard Medical School, 55 Fruit Street, ACC 708, Boston, MA 02114. E-mail: feichler@partners.org

DOI: 10.1089/hum.2018.079

disease, with evidence of sustained transgene expression,[11–13] functional response,[14,15] and an adequate safety profile. In our previous work, we reported both successful transduction of CNS cells and functional reduction of VLCFA accumulation after intravenous delivery of rAAV serotype 9 (rAAV9) vector containing the human *ABCD1* gene (h*ABCD1*).[16]

Systemic intravenous AAV9 delivery was chosen for its ease of injection and its ability to achieve broad distribution of transduction in the CNS. That notwithstanding, systemic delivery requires very large doses of AAV9 to achieve efficient CNS transduction and comes with the possibility of off-target peripheral toxicities and greater exposure to neutralizing anti-AAV antibodies. Therefore, optimizing rAAV delivery to more efficiently target spinal cord and to reduce peripheral leakage became the focus of this study. Intrathecal injection for AAV delivery has been widely used and has the advantage of direct spinal cord exposure.[17,18] In the present study, we compared the efficacy and safety of two different intrathecal infusion speeds (bolus injection and slow delivery using an osmotic pump) to deliver rAAV9-h*ABCD1* in the ALD mouse model. To optimize detection of ABCD1 and better understand its biodistribution, we used hemagglutinin (HA)-tagged ABCD1 to track ABCD1 after AAV9 delivery.

MATERIALS AND METHODS

Cell culture

Human 293T cells were obtained from the American Type Culture Collection (Manassas, VA). Cells were cultured in high-glucose Dulbecco's modified Eagle's medium (DMEM; Invitrogen, Carlsbad, CA) supplemented with 10% fetal bovine serum (FBS) (Sigma-Aldrich, St. Louis, MO) and with penicillin (100 U/mL) and streptomycin (100 μg/mL) (Invitrogen) in a humidified atmosphere supplemented with 5% CO_2 at 37°C.

Animals

Congenic C57BL/6 *Abcd1*$^{-/-}$ and wild-type C57BL/6 mice were bought from Jackson Laboratory (Bar Harbor, ME). *Abcd1*$^{-/-}$ mice were backcrossed onto a pure C57/B6 background over six generations. They were then bred from homozygous founders, and occasionally genotyped according to the protocol provided by Jackson Laboratory. All mice were kept in the animal housing facility of the Massachusetts General Hospital (MGH) Center for Comparative Medicine, had *ad libitum* access to water and standard rodent food, and were kept on a 12-h light and dark cycle. A protocol for early euthanasia/humane endpoints is executed if one of the following criteria is met: the loss of body weight more than 15% or a wound that cannot be improved after medication. All animal experiments were approved by the Institutional Animal Care and Use Committee at MGH.

Recombinant AAV9 vectors

Human *ABCD1* cDNA was kindly provided by J. Berger (University of Vienna) and inserted into the pAAV-CBA vector, using flanking *Hin*dIII and *Xho*I restriction sites (AAV-CBA-h*ABCD1*). This single-stranded rAAV vector contains the strong cytomegalovirus (CMV) enhancer/chicken β-actin hybrid promoter (CBA), a woodchuck hepatitis virus posttranscriptional regulatory element (WPRE), and simian virus 40 (SV40) and bovine growth hormone (BGH) poly(A) sequences. In some of our experiments we utilized an AAV9 capsid carrying an AAV expression cassette encoding green fluorescent protein (GFP) under the control of the CBA promoter (AAV-CBA-*GFP*). AAV-CBA-*GFP* is a self-complementary genome and has been previously described.[19] rAAV production has previously been described.[20] Briefly, 293T cells were transfected with rAAV (pAR9*rep*/*cap* plasmid encoding AAV9 capsid proteins and AAV2-ITR containing transgene [*ABCD1*] expression plasmid [single-stranded genome]) and helper plasmid (pAdΔF6) by the calcium phosphate method. Seventy-two hours posttransfection cells were harvested and vector purified, using a standard iodixanol density gradient and ultracentrifugation protocol. Iodixanol was removed and vector concentrated in phosphate-buffered saline (PBS) by diafiltration using Amicon Ultra 100-kDa MWCO centrifugal devices (Millipore, Billerica, MA). Vector was stored at –80°C until use. rAAV titers were determined by quantitative PCR and expressed as genome copies per milliliter (GC/mL) as described previously.[21] To optimize detection of ABCD1, a C-terminal HA-tagged human *ABCD1* cDNA was separately cloned into pAAV-CBA vector and packaged into rAAV9 in 293T cells. Table 1 outlines the vector constructs, delivery routes, doses, study purpose, and method of analysis used.

Vector administration

Intrathecal osmotic pump (IT pump) delivery. Twelve- to 20-week-old male C57BL/6 *Abcd1*$^{-/-}$ mice were anesthetized with isoflurane. After the skin over the lumbar region was shaved and cleaned, a 3- to 4-cm mid-sagittal incision was made through the skin, exposing the muscle and

Table 1. *Overview of studies*

Vector	*Delivery route*	*Dose*	*Purpose*	*Method of analysis*
Self-complementary rAAV9-CBA-*GFP*	Intrathecal pump	1.5×10^{11} GC/mouse 3×10^{11} GC/mouse	Distribution of GFP across compartments and cell types of the nervous system	Immunofluorescence staining
Single-strand rAAV9-CBA-h*ABCD1*	Intrathecal pump Intrathecal bolus	1×10^{11} GC/mouse	Distribution of ABCD1 in nervous system and peripheral organs Determination of the functionality of rAAV9-CBA-h*ABCD1*	Western blot Lipid analysis by ESI-MS
Single-strand rAAV9-CBA-h*ABCD1*-HA	Intrathecal pump Intrathecal bolus	2×10^{11} GC/mouse	Distribution of ABCD1-HA in nervous system and peripheral organs as well as identifying cell types targeted	Immunofluorescence staining

ABCD1, peroxisomal ATP-binding cassette transporter subfamily D member 1; ESI-MS, electrospray ionization-mass spectrometry; GC, genome copies; GFP, green fluorescent protein; HA, hemagglutinin.

spine. A catheter was inserted into the spine between L4 and L5 and attached to a 2001D mini-osmotic pump (Alzet, Cupertino, CA) containing the rAAV9 vectors in a 200-μL volume. The osmotic pump was implanted under the skin for 24 h and removed the next day.

Intrathecal bolus delivery (IT bolus). Twelve- to 20-week-old male C57BL/6 *Abcd1*$^{-/-}$ mice were anesthetized with isoflurane. After the skin over the lumbar region was shaved and cleaned, a 3- to 4-cm mid-sagittal incision was made through the skin, exposing the muscle and spine. A catheter was inserted into the spine between L4 and L5 and attached to a gas-tight Hamilton syringe with a 33-gauge steel needle. rAAV9 vectors (1×10^{11} GC) in a 10-μL volume were slowly injected at a rate of 2 μL/min.

Tissue and plasma preparation

Fifteen days after injection, mice were anesthetized with isoflurane. Blood was collected from the mice by cardiac puncture and after that the mice were sacrificed by transcardial perfusion of PBS. After removal, brain, liver, spinal cord, and other organ tissues were snap-frozen and stored at –80°C until use. Parts of tissues were fixed with 4% paraformaldehyde (PFA) and equilibrated in 30% sucrose before slicing.

Lipid analysis

To assess the effect of rAAV9-*ABCD1* gene delivery on $C_{22:0}$, $C_{24:0}$, and $C_{26:0}$ levels in liver, spinal cord, and dorsal root ganglia (DRG), fatty acids were analyzed by electrospray ionization-mass spectrometry (ESI-MS) as described previously.[4] Absolute values of $C_{24:0}$ and $C_{26:0}$ are reported as nanomoles per milligram of protein.

Western blotting

Tissue and cell lysates were prepared with RIPA buffer (Sigma-Aldrich) with 1% Halt protease and phosphatase inhibitor cocktail (Roche, Indianapolis, IN). Protein samples were separated on NuPAGE 4–12% Bis-Tris gels (Invitrogen) and transferred on polyvinylidene difluoride (PVDF) membranes. Membranes were blocked with 5% nonfat milk in PBS containing 0.05% Tween 20 and probed with antibody against human ABCD1 (diluted 1:3,000 [Cat. No. ab197013; Abcam, Cambridge, UK]) and HA tag (diluted 1:1,000 [Cat. No. 3724; Cell Signaling, Danvers, MA]) diluted in blocking buffer. Anti-β-actin (diluted 1:1,000 [Cat. No. SC-47778; Santa Cruz Biotechnology, Santa Cruz, CA]) was used as a protein loading control. Membranes were developed with SuperSignal West Pico chemiluminescent substrate (Thermo Scientific, Rockford, IL) after incubation with horseradish peroxidase (HRP)-conjugated secondary antibodies.

Immunofluorescence staining and confocal microscopy imaging

Sections of CNS tissue and peripheral organs (14 μm) were cut at –23°C, using a cryostat (Leica Biosystems, Buffalo Grove, IL). Sections were stained with anti-GFP (diluted 1:200 [Cat. No. G10362; Invitrogen] and diluted 1:1,000 [Cat. No. ab1218; Abcam]), anti-HA (diluted 1:1,600 [Cat. No. 3724; Cell Signaling]), or anti-human ABCD1 (diluted 1:200 [Cat. No. TA803208; OriGene, Rockville, MD]) antibody either separately or in combination with anti-GFAP (glial fibrillary acidic protein, diluted 1:500 [Cat. No. Z0334; Dako, Carpinteria, CA]), anti-IBA1 (ionized calcium binding adapter molecule 1, diluted 1:500 [Cat. No. 019-17841; Wako, Kyoto, Japan]), anti-CD31 (diluted 1:50 [Cat. No. ab28364; Abcam]), anti-Olig2 (oligodendrocyte transcription factor 2, diluted 1:500 [Cat. No. AB9610; Millipore]), anti-SMA (α-smooth muscle actin, diluted 1:100 [Cat. No. ab5694; Abcam]), anti-neurofilament (SMI32, diluted 1:1,000 [Cat. No. 801701; BioLegend, San Diego, CA]), and anti-NeuN (neuronal nuclei, diluted 1:1,000 [Cat. No. ab104224; Abcam]) to localize the cell type. The slides were imaged by confocal laser microscopy.

Mouse brain glial cell culture and rAAV9-CBA-hABCD1-HA transduction

Primary brain glial cell mixed culture was performed as follows. Briefly, 2- to 3-day-old *Abcd1*$^{-/-}$

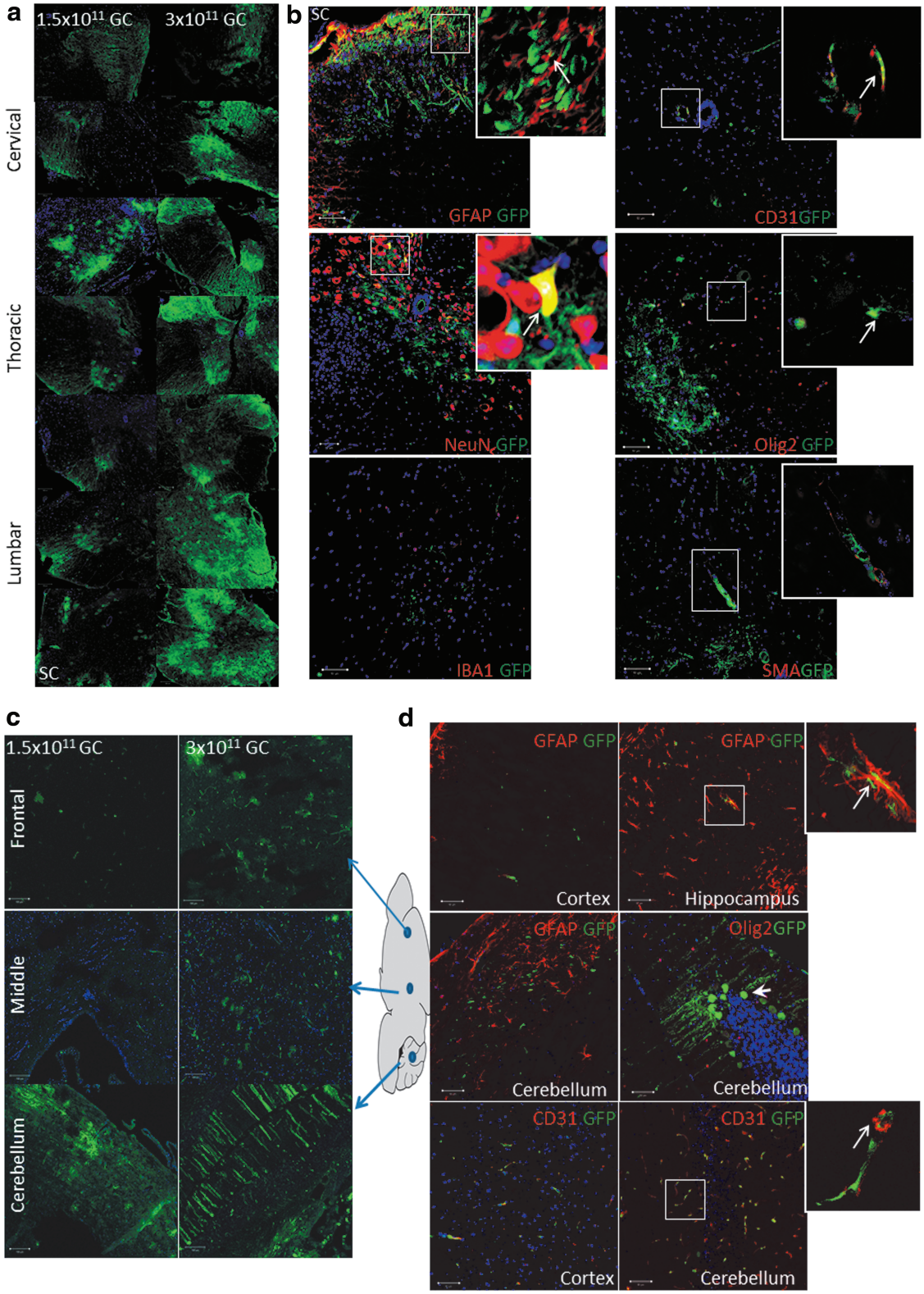

Figure 1. Green fluorescent protein (GFP) expression across the mouse nervous system after intrathecal osmotic pump delivery, and cell types transduced. **(a)** Dose-dependent rAAV9-CBA-*GFP* expression in the spinal cord after intrathecal osmotic pump (IT pump) delivery at 1.5×10^{11} and 3×10^{11} genome copies (GC). **(b)** Cell types targeted in the spinal cord after IT pump delivery identified by costaining with various cellular markers including GFAP (glial fibrillary acidic protein; astrocytes), IBA1 (ionized calcium binding adapter molecule 1; microglia), CD31 (endothelial cells), NeuN (neuronal nuclei; neurons), Olig2 (oligodendrocyte transcription factor 2; oligodendrocytes), and SMA (α-smooth muscle actin; smooth muscle cells). **(c)** Dose-dependent rAAV9-CBA-*GFP* expression in the brain after IT pump delivery at 1.5×10^{11} and 3×10^{11} GC. **(d)** Cell types targeted in the brain after IT delivery, identified by costaining with various cellular markers. *Thick short-stemmed white arrow* indicates a neuron targeted. *Blue arrows* indicate where the image is taken from brain anatomy. **(e)** Dose-dependent rAAV9-CBA-*GFP* expression in dorsal root ganglia (DRG) seen in various regions after IT pump delivery at 1.5×10^{11} and 3×10^{11} GC, as well as cell types targeted. These are identified by costaining with neuronal markers NeuN and neurofilament (NF). *Thin long-stemmed white arrows* in each panel indicate co-stained cells. PBS, phosphate-buffered saline. Color images are available online.

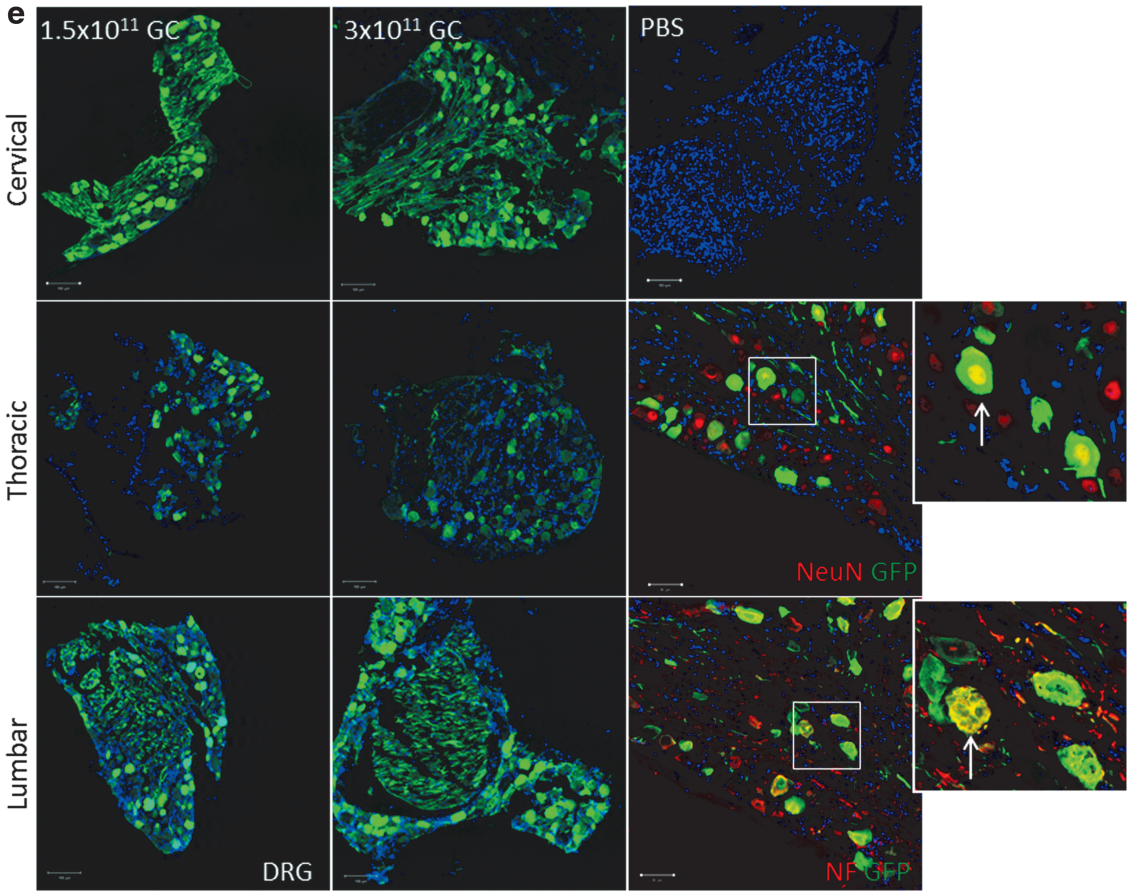

Figure 1. (Continued)

pups ($n = 4$) were sacrificed; the brain was dissected and hindbrain removed. After washing twice with PBS, brain tissue was incubated with 0.05% trypsin for 10 min followed by a 5-min incubation in DNase I. Digested brain tissues were triturated with a 1-mL pipette and passed over a 100-μm filter. Filtered cells were collected by centrifuge, suspended in DMEM containing 10% FBS, and cultured in T75 flasks at 37°C until confluent. Brain cells were passed onto 6-well plates for 24 h and transduced with various doses of rAAV9-*ABCD1*-HA for 5 days. Cells were then fixed in 4% PFA for immunofluorescence staining of HA tag and ABCD1.

Statistics

Results are expressed as means ± SEM and were analyzed for statistical significance by analysis of variance (ANOVA) followed by Fisher's protected least-significant difference based on two-side comparisons among experimental groups, using the SPSS program (IBM, Armonk, NY). $p < 0.05$ was considered statistically significant.

RESULTS

Intrathecal delivery of rAAV9-CBA-*GFP* with osmotic pump leads to widespread expression in nervous system and cell types targeted

To test the feasibility of AAV9-mediated gene delivery by osmotic pump, we performed intrathecal delivery of self-complementary rAAV9-CBA-*GFP* with an osmotic pump over a duration of 24 h. We examined two different doses of rAAV9-CBA-*GFP* at 1.5×10^{11} and 3×10^{11} GC/mouse. A dose-dependent increase in GFP expression was detected across the spinal cord and brain (Fig. 1a and c). To further determine the cell type transduced, we costained GFP with various cellular markers including GFAP (astrocytes), IBA1 (microglia), CD31 (endothelial cells), NeuN (neurons), Olig2 (oligodendrocytes), and SMA (smooth muscle cells). As shown in Fig. 1b, rAAV9-CBA-*GFP* injected via IT pump targeted mainly astrocytes, vascular endothelial cells, and neurons in the spinal cord. Microglial transduction was not detected. In brain, cellular markers showed that astrocytes, endothelial cells, and neurons were the main target cell types (Fig. 1d). In DRG tissue,

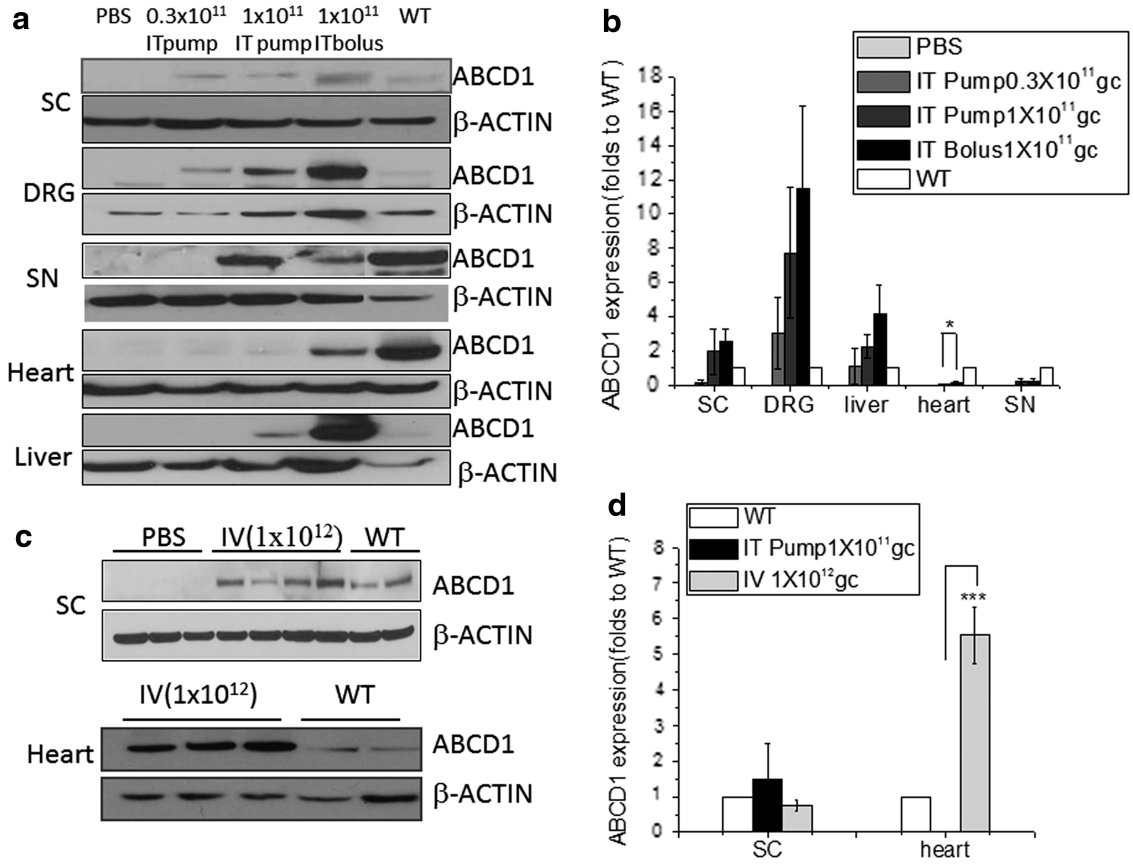

Figure 2. Distribution of ABCD1 protein after intrathecal delivery of rAAV9-CBA-h*ABCD1*. **(a)** Representative Western blot images show ABCD1 expression in various organs of *Abcd1*$^{-/-}$ mice after intrathecal osmotic pump (IT pump) and intrathecal bolus (IT bolus) delivery at various vector doses and **(b)** quantification of protein intensity after normalization to β-actin. **(c)** Representative Western blot images show rAAV9-CBA-h*ABCD1* expression in various organs after intravenous (IV) injection in spinal cord and heart tissue and **(d)** protein intensity comparison between IT pump and IV injection. Results are expressed as means ± SEM of the various animals: $^{*}p<0.05$, $^{***}p<0.001$. ABCD1, peroxisomal ATP-binding cassette transporter subfamily D member 1; GC, genome copies; DRG, dorsal root ganglia; PBS, phosphate-buffered saline; SC, spinal cord; SN, sciatic nerve; WT, wild type.

higher doses increased GFP expression, mainly within DRG neurons (Fig. 1e).

Distribution of ABCD1 protein after intrathecal delivery of rAAV9-CBA-h*ABCD1*

We next set out to test the distribution of our therapeutic protein, hABCD1, after intrathecal delivery of rAAV9-CBA-h*ABCD1*. As shown in Fig. 2a and b, IT bolus and IT pump delivery at 1×10^{11} GC/mouse both led to ABCD1 expression in spinal cord and DRG. In rodent brain expression of ABCD1 was limited and detected only at the higher dose (3×10^{11} GC/mouse; Supplementary Fig. S1). In spinal cord, with either delivery method and with rAAV9-*ABCD1* at 1×10^{11} GC/mouse, the ABCD1 protein expression level was comparable to the wild-type ABCD1 expression level. In DRG, with rAAV9-CBA-*ABCD1* at 1×10^{11} GC/mouse, the ABCD1 protein expres-

Figure 3. Distribution and cell types immunoreactive for HA-tagged ABCD1 after intrathecal delivery of rAAV9-CBA-h*ABCD1*-HA. **(a)** Colocalization of HA tag with ABCD1 after rAAV9-CBA-h*ABCD1*-HA transduction at 5×10^{5} GC/cell in mixed glial cell culture. **(b)** Representative images show rAAV9-CBA-h*ABCD1*-HA distribution across the whole spinal cord after IT pump and IT bolus delivery at 2×10^{11} GC/mouse. Higher magnification image shows punctate HA tag expression (HA, green) in glial cells and some neurons (NF, *red*). **(c)** Representative images show rAAV9-CBA-h*ABCD1*-HA distribution across DRGs after IT pump and IT bolus delivery at 2×10^{11} GC/mouse. Higher magnification image shows punctate HA tag expression (HA, green) in DRG neurons (NF, *red*). **(d)** Cell types targeted in the spinal cord after IT delivery identified by costaining with various cellular markers including GFAP (astrocytes), IBA1 (microglia), NeuN (neurons), and Olig2 (oligodendrocytes) (HA, red). **(e)** Representative images show rAAV9-CBA-h*ABCD1*-HA distribution in peripheral organs after IT pump and IT bolus delivery at 2×10^{11} GC/mouse. ABCD1, peroxisomal ATP-binding cassette transporter subfamily D member 1; DRG, dorsal root ganglia; GC, genome copies; GFAP, glial fibrillary acidic protein; HA, hemagglutinin; IBA1, ionized calcium binding adapter molecule 1; IT, intrathecal; NeuN, neural nuclei; NF, neurofilament; Olig2, oligodendrocyte transcription factor 2; SC, spinal cord. Color images are available online.

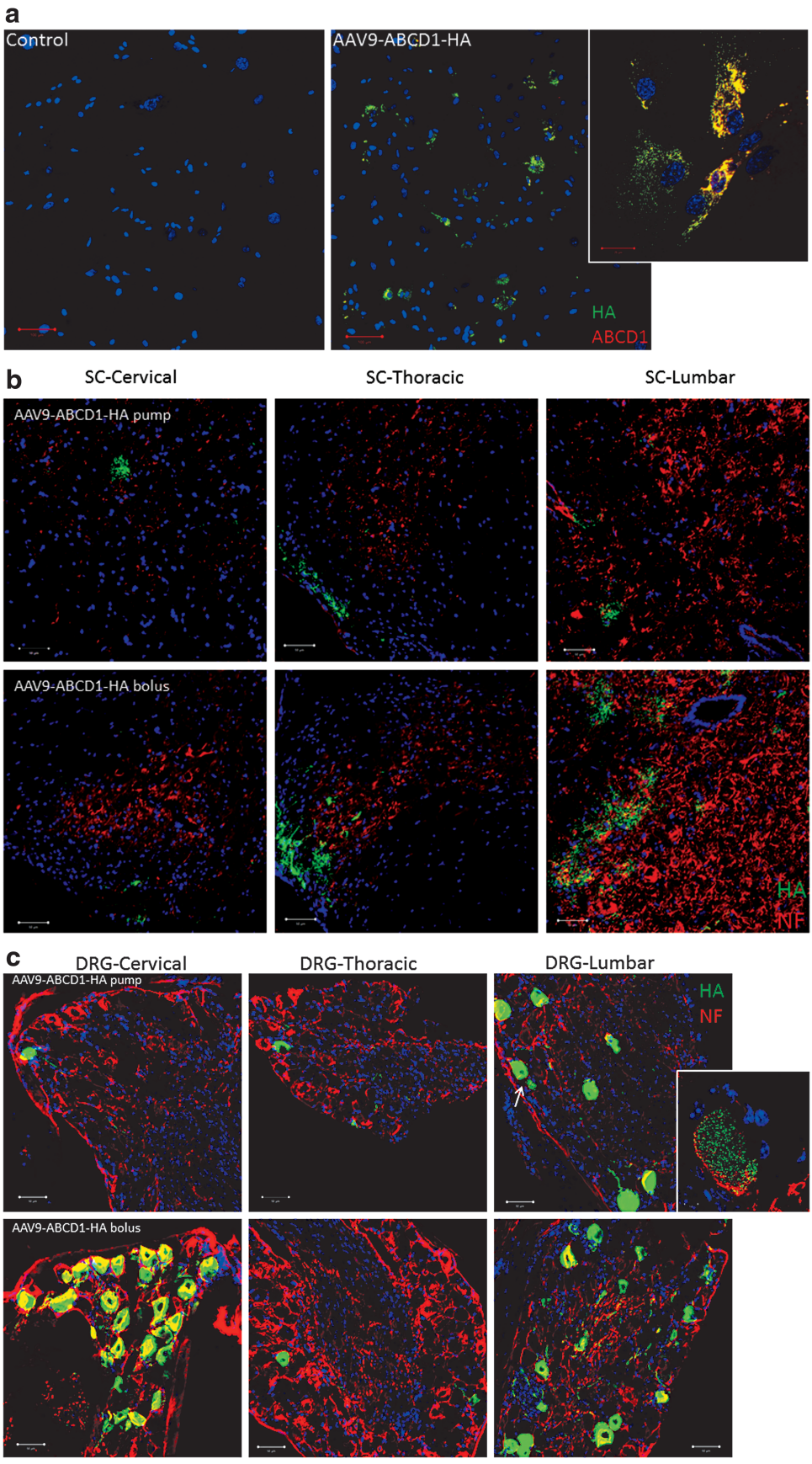
a
Control
AAV9-ABCD1-HA
HA
ABCD1
b
SC-Cervical
SC-Thoracic
SC-Lumbar
AAV9-ABCD1-HA pump
AAV9-ABCD1-HA bolus
HA
NF
c
DRG-Cervical
DRG-Thoracic
DRG-Lumbar
AAV9-ABCD1-HA pump
AAV9-ABCD1-HA bolus
HA
NF

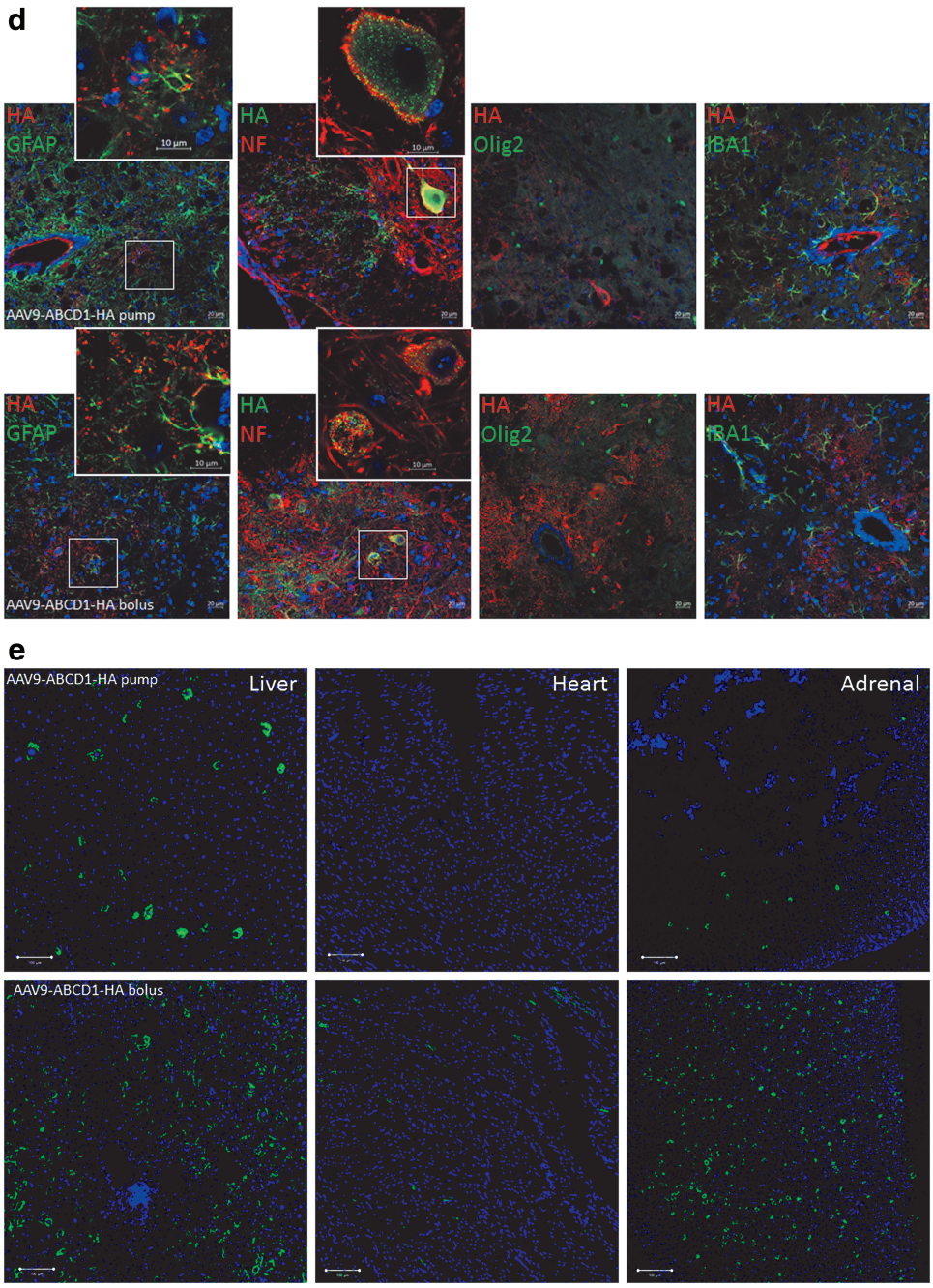

Figure 3. (Continued)

sion level was about 5- to 10-fold higher than the expression level in wild-type mice. With both delivery methods, a small amount of ABCD1 protein was also detected in sciatic nerve (SN) tissue.

Expression of ABCD1 protein was also found in peripheral organs (heart and liver) after intrathecal delivery. However, compared with bolus injection, IT osmotic pump delivery significantly reduced systemic leakage particularly in heart tissue (Fig. 2a and b; $p < 0.05$). Compared with intravenous injection at 1×10^{12} GC/mouse, a slightly higher expression of ABCD1 protein was achieved in the spinal cord via IT osmotic pump delivery. Not unexpectedly, IT pump delivery led to significant reductions ($p < 0.001$) of ABCD1 protein expression in heart compared with intravenous delivery, evidence of minimized peripheral leakage (Fig. 2c and d).

Tracking ABCD1 after intrathecal delivery using rAAV9-CBA-h*ABCD1*-HA

Because of the lack of an ABCD1 antibody with high specificity for *in vivo* immunostaining, we

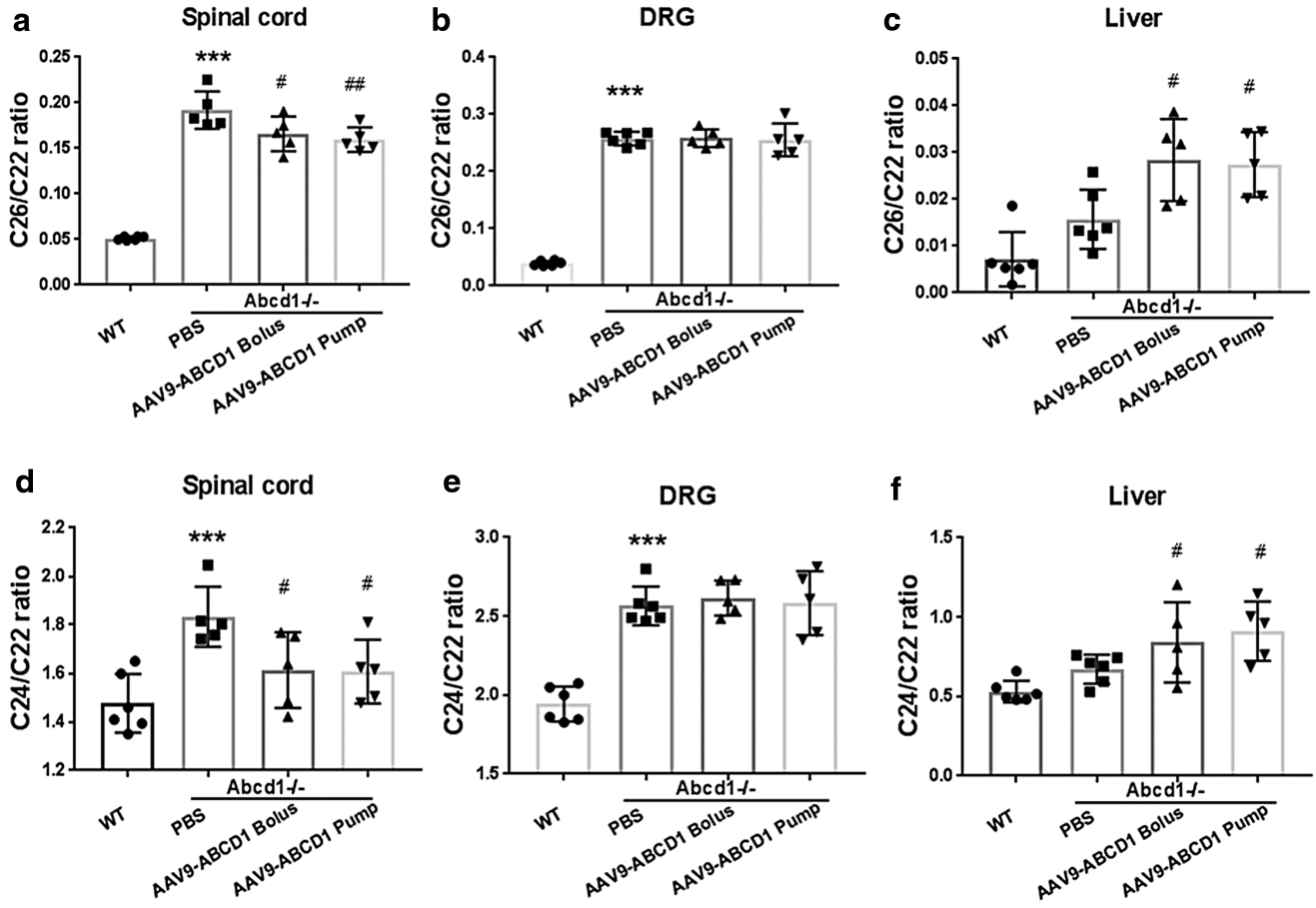

Figure 4. Intrathecal injection of rAAV9-CBA-h*ABCD1* leads to partial biochemical correction in *Abcd1*$^{-/-}$ mouse spinal cord. **(a–c)** $C_{26:0}$ levels in spinal cord, DRG, and liver after intrathecal osmotic pump (IT pump) and intrathecal bolus (IT bolus) delivery of rAAV9-CBA-h*ABCD1* at 1×10^{11} GC/mouse. **(d–f)** $C_{24:0}$ levels in spinal cord, DRG, and liver after intrathecal osmotic pump and bolus delivery at 1×10^{11} GC/mouse. Data are expressed as means ± SEM. $^{***}p<0.001$ compared with wild type; $^{\#}p<0.05$, $^{\#\#}p<0.01$ compared with PBS control. DRG, dorsal root ganglia; GC, genome copies; PBS, phosphate-buffered saline; WT, wild type.

generated rAAV9-CBA-h*ABCD1* with a C-terminal HA tag (rAAV9-CBA-h*ABCD1*-HA). *In vitro* transduction in mixed glial cells at 5×10^5 GC/cell showed exact colocalization of the HA tag with the ABCD1 protein (Fig. 3a), indicating the feasibility to track ABCD1 distribution by HA tag immunostaining. Intrathecal delivery of 2×10^{11} GC of rAAV9-CBA-h*ABCD1*-HA to mice revealed widespread, yet sparse distribution across various parts of spinal cord (Fig. 3b) and DRG (Fig. 3c) in either the IT pump- or IT bolus-injected group. Costaining with various cellular markers revealed punctate protein expressed largely in astrocytes and neurons in spinal cord (Fig. 3d) but mainly neurons in DRG (Fig. 3c), consistent with the result seen after rAAV9-CBA-*GFP* delivery. Immunostaining in peripheral tissues revealed liver, heart, and adrenal gland as the major organs transduced after intrathecal delivery of rAAV9-CBA-h*ABCD1*-HA. IT pump delivery reduced systemic leakage compared with IT bolus (Fig. 3e), further corroborating the results from Western blotting (Fig. 2).

Intrathecal injection of rAAV9-CBA-h*ABCD1* leads to biochemical correction in spinal cord

To determine the functionality of rAAV9-CBA-h*ABCD1* delivered intrathecally, we collected tissue from mice 15 days after undergoing rAAV9-CBA-h*ABCD1* injection. A 17% reduction in $C_{26:0}$ level was detected in spinal cord after IT osmotic pump delivery (1×10^{11} GC/mouse) whereas a 15% reduction was detected after bolus injection (Fig. 4 and Supplementary Fig. S2 for AAV9-Empty vector control). Levels of $C_{24:0}$ showed a similar trend. Unexpectedly, the $C_{26:0}$ level in DRG remained unchanged after intrathecal delivery (Fig. 4) despite the robust increase in ABCD1 protein expression in DRG neurons (Figs. 2 and 3). In the liver, an increase in $C_{26:0}$ was observed that may have been related

to local inflammation, in turn related to vector transduction[22] (Fig. 4). The purity and functionality of rAAV9-CBA-hABCD1 was shown in Supplementary Figure S3.

DISCUSSION

Attaining efficient and uniform delivery of targeted therapy for a neurological disorder has been a longstanding challenge. This is pertinent to AMN, which has few systemic manifestations and relative selective involvement of spinal cord and DRG. Current cell-based therapies, such as bone marrow transplantation and *ex vivo* gene therapy, although halting brain manifestations, appear limited in their capacity to ameliorate AMN.[8,10]

In the present study, we achieved efficient delivery of rAAV9-CBA-*GFP* to the spinal cord and DRG by lumbar 24-h intrathecal infusion using an osmotic pump. By the same approach we further report reducing $C_{26:0}$ levels by 20% in the spinal cord of *Abcd1*$^{-/-}$ mice receiving rAAV9-CBA-h-*ABCD1*. Importantly, this delivery method reduced systemic leakage into peripheral organs, particularly into liver and heart tissue. Immunofluorescence staining with various cellular markers revealed that astrocytes, vascular endothelial cells, and neurons were the major cell types targeted.

As there have been no reports on lowering spinal cord $C_{26:0}$ to date, it is currently unclear whether a 20% reduction would lead to a clinical benefit. The aforementioned cell-based therapies do not lower plasma VLCFA and yet stabilize demyelination in brain, likely by rescuing key inflammatory cells. Future studies will need to show whether our intrathecal gene delivery provides a benefit to the late-onset behavioral phenotype in *Abcd1*$^{-/-}$ mice.

Although safe intravenous administration of AAV9 has occurred even in humans,[23,24] some studies have reported evidence of transgene-specific toxicity in peripheral organs.[25,26] Specifically, we and others have found that intravenous delivery of AAV9 leads to high transgene expression in the heart tissue of mice.[16,24,27] Systemic delivery also requires administration of higher quantities of vectors to attain comparable outcomes, posing a challenge to manufacturing capacity during commercialization.

Across various species intrathecal delivery has been found to be more efficient than intravenous delivery in transducing spinal cord and DRG.[27,28] Widespread transgene expression throughout the spinal cord was already seen in both mice and nonhuman primates with a dosage 10-fold lower than the dosage used for intravenous administration.[28] Whereas in rodents intrathecal AAV delivery produced only minimal brain transduction[29–34] (Supplementary Fig. S1), in pigs a high degree of brain transduction was present regardless of whether the vector was injected diffusely across the spinal cord or into the lumbar cistern (S.J. Gray, unpublished data; mentioned in Reference 35). In nonhuman primates, vascular delivery of AAV9-GFP to the brain was weaker compared with the signal seen in animals that received AAV9-GFP via the cisterna magna.[36] These studies suggest that injection into cerebrospinal fluid (CSF) has the potential for widespread transduction of the brain and spinal cord, allowing studies to be scaled up to larger animals and humans.

Although largely unexplored, infusion speed may be an important determinant in optimizing the delivery of AAV-mediated gene correction. Slow administration may help reduce leakage into the vascular compartment, a phenomenon that we encountered after bolus injections. This is evidenced by the most recent report from Li and co-workers that slow intrathecal injection of rAAVrh10 enhances its transduction of spinal cord and therapeutic efficacy in a mutant superoxide dismutase 1 (SOD1) model of amyotrophic lateral sclerosis (ALS).[37] Increased knowledge and experience with respect to the mechanics of flow speed and the barrier function within the CSF compartment, already exploited in the field of anesthesia, will help shape studies in human subjects.

Wang and colleagues have used intrathecal delivery of a self-complementary AAV9 encoding GFP via osmotic pump in mice and, similar to our results with AAV9-GFP (Fig. 1), transduction was robust throughout the entire spinal cord.[38] Although we readily detected AAV-mediated ABCD1 expression after osmotic pump delivery by both Western blotting and immunofluorescence staining (Figs. 2 and 3), transgene-positive cells were much more diffuse for ABCD1 (Fig. 3b and c) than for GFP (Fig. 1a–e). A possible explanation for this is the use of a single-stranded genome for the ABCD1 expression cassette versus a self-complementary cassette for GFP expression. Another explanation could involve differences in immunofluorescence detection of GFP and ABCD1. GFP has natural fluorescence, which is magnified by immunofluorescence staining. This is not the case for ABCD1. Furthermore, the C-terminal HA tag may not be accessible on all vector-expressed molecules of ABCD1.

Both pump and bolus injections achieved transgene expression in spinal cord and DRG in the same cell types, and the osmotic pump consistently reduced transgene expression in peripheral tissues, an important consideration for future safety studies. Both intrathecal pump and bolus injections of AAV9-ABCD1 led to VLCFA reduction

(~20%) in the spinal cord (Fig. 4). The fact that many of the cells transduced in spinal cord (*e.g.*, glial cells) endogenously express ABCD1 points to the relevance of our approach in reconstituting the normal biological distribution.

Although high expression of transgene was detected in DRG neurons in mice injected intrathecally (Figs. 1e and 3c), little expression was detected in satellite glial cells (SGCs). Endogenous ABCD1 expression, although only sparsely present in neurons, is more highly expressed in SGCs (data not shown). The fact that we do not achieve robust transduction of SGCs with intrathecally delivered AAV9-ABCD1 likely explains the lack of VLCFA reduction in DRG tissue (Fig. 4). Future strategies aimed at improving transduction of SGCs may enable lowering of VLCFA in DRG. Furthermore, SGC studies in nonhuman primates are necessary to corroborate whether this tropism in mice is relevant to larger animals and humans. We also note that our intrathecal AAV9-*ABCD1* infusions led to elevations in very long-chain fatty acids in the liver, an organ usually not involved in AMN. Although we did not observe any subsequent pathology, this may require monitoring in future trials.

In conclusion, we demonstrate in a mouse model of AMN that intrathecal osmotic pump delivery is an efficient and promising strategy for AAV9-mediated expression of ABCD1 protein in the spinal cord. Compared with intravenous injection and bolus intrathecal injection, slow delivery of vector via osmotic pump reduced systemic leakage, especially to the heart, while still being able to lower VLCFA levels in the spinal cord. Further testing in nonhuman primates may enable the development of intrathecal AAV9-*ABCD1* as a gene therapy for AMN.

ACKNOWLEDGMENTS

This work was supported by grants from the Leblang Charitable Foundation, the Myelin Project, the University of Pennsylvania Orphan Disease Center, Applied Genetic Technologies Corporation, and the NIH (R01 NINDS).

AUTHOR DISCLOSURE

C.A.M. and F.E. are both inventors on a patent application that covers *ABCD1* gene delivery with AAV vectors described in this article.

REFERENCES

1. Mosser J, Douar AM, Sarde CO, et al. Putative X-linked adrenoleukodystrophy gene shares unexpected homology with ABC transporters. Nature 1993;361:726–730.
2. van Roermund CW, Visser WF, Ijlst L, et al. The human peroxisomal ABC half transporter ALDP functions as a homodimer and accepts acyl-CoA esters. FASEB J 2008;22:4201–4208.
3. Moser AB, Kreiter N, Bezman L, et al. Plasma very long chain fatty acids in 3,000 peroxisome disease patients and 29,000 controls. Ann Neurol 1999;45:100–110.
4. Valianpour F, Selhorst JJ, van Lint LE, et al. Analysis of very long-chain fatty acids using electrospray ionization mass spectrometry. Mol Genet Metab 2003;79:189–196.
5. Moser HW. Adrenoleukodystrophy: phenotype, genetics, pathogenesis and therapy. Brain 1997; 120:1485–1508.
6. Engelen M, Barbier M, Dijkstra IM, et al. X-linked adrenoleukodystrophy in women: a cross-sectional cohort study. Brain 2014;137:693–706.
7. Cartier N, Hacein-Bey-Abina S, Bartholomae CC, et al. Hematopoietic stem cell gene therapy with a lentiviral vector in X-linked adrenoleukodystrophy. Science 2009;326:818–823.
8. Eichler F, Duncan C, Musolino PL, et al. Hematopoietic stem-cell gene therapy for cerebral adrenoleukodystrophy. N Engl J Med 2017;377: 1630–1638.
9. Kemp S, Huffnagel IC, Linthorst GE, et al. Adrenoleukodystrophy: neuroendocrine pathogenesis and redefinition of natural history. Nat Rev Endocrinol 2016;12:606–615.
10. van Geel BM, Poll-The BT, Verrips A, et al. Hematopoietic cell transplantation does not prevent myelopathy in X-linked adrenoleukodystrophy: a retrospective study. J Inher Metab Dis 2015;38: 359–361.
11. Kaplitt MG, Feigin A, Tang C, et al. Safety and tolerability of gene therapy with an adeno-associated virus (AAV) borne GAD gene for Parkinson's disease: an open label, phase I trial. Lancet 2007;369:2097–2105.
12. Marks WJ Jr, Ostrem JL, Verhagen L, et al. Safety and tolerability of intraputaminal delivery of CERE-120 (adeno-associated virus serotype 2-neurturin) to patients with idiopathic Parkinson's disease: an open-label, phase I trial. Lancet Neurol 2008;7:400–408.
13. Worgall S, Sondhi D, Hackett NR, et al. Treatment of late infantile neuronal ceroid lipofuscinosis by CNS administration of a serotype 2 adeno-associated virus expressing CLN2 cDNA. Hum Gene Ther 2008;19:463–474.
14. Nathwani AC, Tuddenham EG, Rangarajan S, et al. Adenovirus-associated virus vector-mediated gene transfer in hemophilia B. N Engl J Med 2011;365: 2357–2365.
15. Maguire AM, High KA, Auricchio A, et al. Age-dependent effects of RPE65 gene therapy for Leber's congenital amaurosis: a phase 1 dose-escalation trial. Lancet 2009;374:1597–1605.
16. Gong Y, Mu D, Prabhakar S, et al. Adenoassociated virus serotype 9-mediated gene therapy for X-linked adrenoleukodystrophy. Mol Ther 2015;23: 824–834.
17. Wang H, Yang B, Qiu L, et al. Widespread spinal cord transduction by intrathecal injection of rAAV delivers efficacious RNAi therapy for amyotrophic lateral sclerosis. Hum Mol Genet 2014;23:668–681.
18. Hirai T, Enomoto M, Machida A, et al. Intrathecal shRNA-AAV9 inhibits target protein expression in the spinal cord and dorsal root ganglia of adult mice. Hum Gene Ther Methods 2012;23:119–127.
19. Gyorgy B, Sage C, Indzhykulian AA, et al. Rescue of hearing by gene delivery to inner-ear hair cells using exosome-associated AAV. Mol Ther 2017; 25:379–391.
20. Maguire CA, Meijer DH, LeRoy SG, et al. Preventing growth of brain tumors by creating a zone of resistance. Mol Ther 2008;16:1695–1702.
21. Maguire CA, Balaj L, Sivaraman S, et al. Microvesicle-associated AAV vector as a novel gene delivery system. Mol Ther 2012;20:960–971.

22. Breous E, Somanathan S, Bell P, et al. Inflammation promotes the loss of adeno-associated virus-mediated transgene expression in mouse liver. Gastroenterology 2011;141:348–357, 357.e341–343.

23. Murrey DA, Naughton BJ, Duncan FJ, et al. Feasibility and safety of systemic rAAV9-hNAGLU delivery for treating mucopolysaccharidosis IIIB: toxicology, biodistribution, and immunological assessments in primates. Hum Gene Ther Clin Dev 2014;25:72–84.

24. Chen BD, He CH, Chen XC, et al. Targeting transgene to the heart and liver with AAV9 by different promoters. Clin Exp Pharmacol Physiol 2015;42:1108–1117.

25. Gadalla KK, Bailey ME, Spike RC, et al. Improved survival and reduced phenotypic severity following AAV9/MECP2 gene transfer to neonatal and juvenile male Mecp2 knockout mice. Mol Ther 2013; 21:18–30.

26. Sun CP, Wu TH, Chen CC, et al. Studies of efficacy and liver toxicity related to adeno-associated virus-mediated RNA interference. Hum Gene Ther 2013;24:739–750.

27. Guo Y, Wang D, Qiao T, et al. A single injection of recombinant adeno-associated virus into the lumbar cistern delivers transgene expression throughout the whole spinal cord. Mol Neurobiol 2016;53:3235–3248.

28. Meyer K, Ferraiuolo L, Schmelzer L, et al. Improving single injection CSF delivery of AAV9-mediated gene therapy for SMA: a dose-response study in mice and nonhuman primates. Mol Ther 2015;23:477–487.

29. Storek B, Harder NM, Banck MS, et al. Intrathecal long-term gene expression by self-complementary adeno-associated virus type 1 suitable for chronic pain studies in rats. Mol Pain 2006;2:4.

30. Storek B, Reinhardt M, Wang C, et al. Sensory neuron targeting by self-complementary AAV8 via lumbar puncture for chronic pain. Proc Natl Acad Sci U S A 2008;105:1055–1060.

31. Kao JH, Chen SL, Ma HI, et al. Intrathecal delivery of a mutant micro-opioid receptor activated by naloxone as a possible antinociceptive paradigm. J Pharmacol Exp Ther 2010;334:739–745.

32. Snyder BR, Gray SJ, Quach ET, et al. Comparison of adeno-associated viral vector serotypes for spinal cord and motor neuron gene delivery. Hum Gene Ther 2011;22:1129–1135.

33. Towne C, Pertin M, Beggah AT, et al. Recombinant adeno-associated virus serotype 6 (rAAV2/6)-mediated gene transfer to nociceptive neurons through different routes of delivery. Mol Pain 2009;5:52.

34. Vulchanova L, Schuster DJ, Belur LR, et al. Differential adeno-associated virus-mediated gene transfer to sensory neurons following intrathecal delivery by direct lumbar puncture. Mol Pain 2010;6:31.

35. Gray SJ, Nagabhushan Kalburgi S, McCown TJ, et al. Global CNS gene delivery and evasion of anti-AAV-neutralizing antibodies by intrathecal AAV administration in non-human primates. Gene Ther 2013;20:450–459.

36. Samaranch L, Salegio EA, San Sebastian W, et al. Adeno-associated virus serotype 9 transduction in the central nervous system of nonhuman primates. Hum Gene Ther 2012;23:382–389.

37. Li D, Liu C, Yang C, et al. Slow intrathecal injection of rAAVrh10 enhances its transduction of spinal cord and therapeutic efficacy in a mutant SOD1 model of ALS. Neuroscience 2017;365:192–205.

38. Wang D, Li J, Tran K, et al. Slow infusion of recombinant adeno-associated viruses into the mouse cerebrospinal fluid space. Hum Gene Ther Methods 2018;29:75–85.

Received for publication April 16, 2018;
accepted after revision October 23, 2018.

Published online: October 24, 2018.